Characterisation of bacterial decay effects on wooden foundation piles across various historical periods

Mirra, Michele; Pagella, Giorgio; Lee, Michael; Gard, Wolfgang; Ravenshorst, Geert; van de Kuilen, Jan Willem

DOI
10.1016/j.conbuildmat.2024.135670

Publication date
2024

Document Version
Final published version

Published in
Construction and Building Materials

Citation (APA)
Mirra, M., Pagella, G., Lee, M., Gard, W., Ravenshorst, G., & van de Kuilen, J. W. (2024). Characterisation of bacterial decay effects on wooden foundation piles across various historical periods. *Construction and Building Materials*, *421*, Article 135670. https://doi.org/10.1016/j.conbuildmat.2024.135670

Construction and Building Materials 421 (2024) 135670

Contents lists available at ScienceDirect

Construction and Building Materials

journal homepage: www.elsevier.com/locate/conbuildmat

Characterisation of bacterial decay effects on wooden foundation piles across various historical periods

Michele Mirra [a,*], Giorgio Pagella [a], Michael Lee [a], Wolfgang Gard [a], Geert Ravenshorst [a], Jan-Willem van de Kuilen [a,b]

[a] Department of Engineering Structures, Section of Biobased Structures and Materials, Delft University of Technology, Stevinweg 1, Delft 2628 CN, the Netherlands
[b] Department of Wood Technology, Technical University of Munich, Winzererstrasse 45, Munich 80797, Germany

ARTICLE INFO

Keywords:
Wooden foundation piles
Bacterial decay
Micro-drilling techniques
Service life modelling
Conservation of architectural heritage

ABSTRACT

In the historic city centre of Amsterdam (NL), the predominant foundation system is comprised of wooden piles. Due to their placement below the water table, these foundations are susceptible to bacterial decay. This study aims to investigate and compare various methods for characterizing decay patterns within the cross sections of piles retrieved from two bridges in Amsterdam. The examined piles span different construction years: three originate from 1727, four from 1886, and two from 1922. Following extraction, the piles were transported to TU Delft Stevin II Laboratory, where they underwent further subdivision into three segments, each representing the head, middle, and tip, resulting in a total of 27 segments. The effects of bacterial decay were characterised by performing micro-drilling measurements, small-scale material and compressive tests on prismatic samples extracted from the segments' cross sections, computed tomography scans, and light microscopy observations. Microscopic examination revealed severe degradation in all segments dating back to 1727, extending 20–50 mm from their surface. This outcome was also confirmed by the other adopted methods: the corresponding prisms had large moisture contents and poor mechanical properties, while low basic densities and drilling amplitudes were obtained from CT scans and micro-drilling measurements, respectively. On the contrary, the internal sections of the 1727 segments exhibited no evidence of decay and demonstrated properties consistent with those observed in sound segments from 1886 and 1922. Finally, the observed gradients of density, strength, and stiffness were well correlated with micro-drilling measurements, which can therefore be reliably used as on-site assessment method to reconstruct the properties of the piles.

1. Introduction

1.1. Background

The utilization of wooden piles as foundation system of historical or existing buildings has been widespread throughout Europe. In this context, the city of Amsterdam (NL) constitutes one of the reference examples for such foundation structures, since it was built on millions of wooden piles, still supporting existing and historical buildings as well as bridges and quay walls. When wooden foundation piles in ground are subjected to biological decay, their load-carrying capacity can be strongly reduced, leading to stability issues in the supported buildings. Since the piles are located below the water table, they can benefit from a longer service life [1–6]: microbial decay of wooden foundations in waterlogged soils can be caused by either soft rot fungi (in low-oxygen conditions), or bacteria (even in anoxic conditions) [4,7]. The latter biodegradation type proceeds more slowly over time than fungal attack. These bacteria, named erosion bacteria on the basis of their way of eroding the wood fibre cell walls [8,9], are responsible for wood degradation in all types of waterlogged anaerobic terrestrial and marine environments worldwide [1,4,10–16], and are able to deeply penetrate into the wood matrix, destroying cellulose and hemicelluloses [1,4].

In particular, spruce (*Picea abies*) and pine (*Pinus sylvestris*) wooden foundation piles degraded by erosion bacteria appear unaffected when examined on site, because their surface, layer, colour, and original dimensions are maintained in wet conditions [6,7]. However, the outer layer could often be soft and spongy because of the degradation, which always starts involving the less durable sapwood, whereas the inner part of the pile, including heartwood, might be less decayed or even sound [1,4,6,7,17,18]. These differences in degradation within the cross

* Corresponding author.
E-mail address: M.Mirra@tudelft.nl (M. Mirra).

https://doi.org/10.1016/j.conbuildmat.2024.135670
Received 16 January 2024; Received in revised form 26 February 2024; Accepted 29 February 2024
Available online 7 March 2024

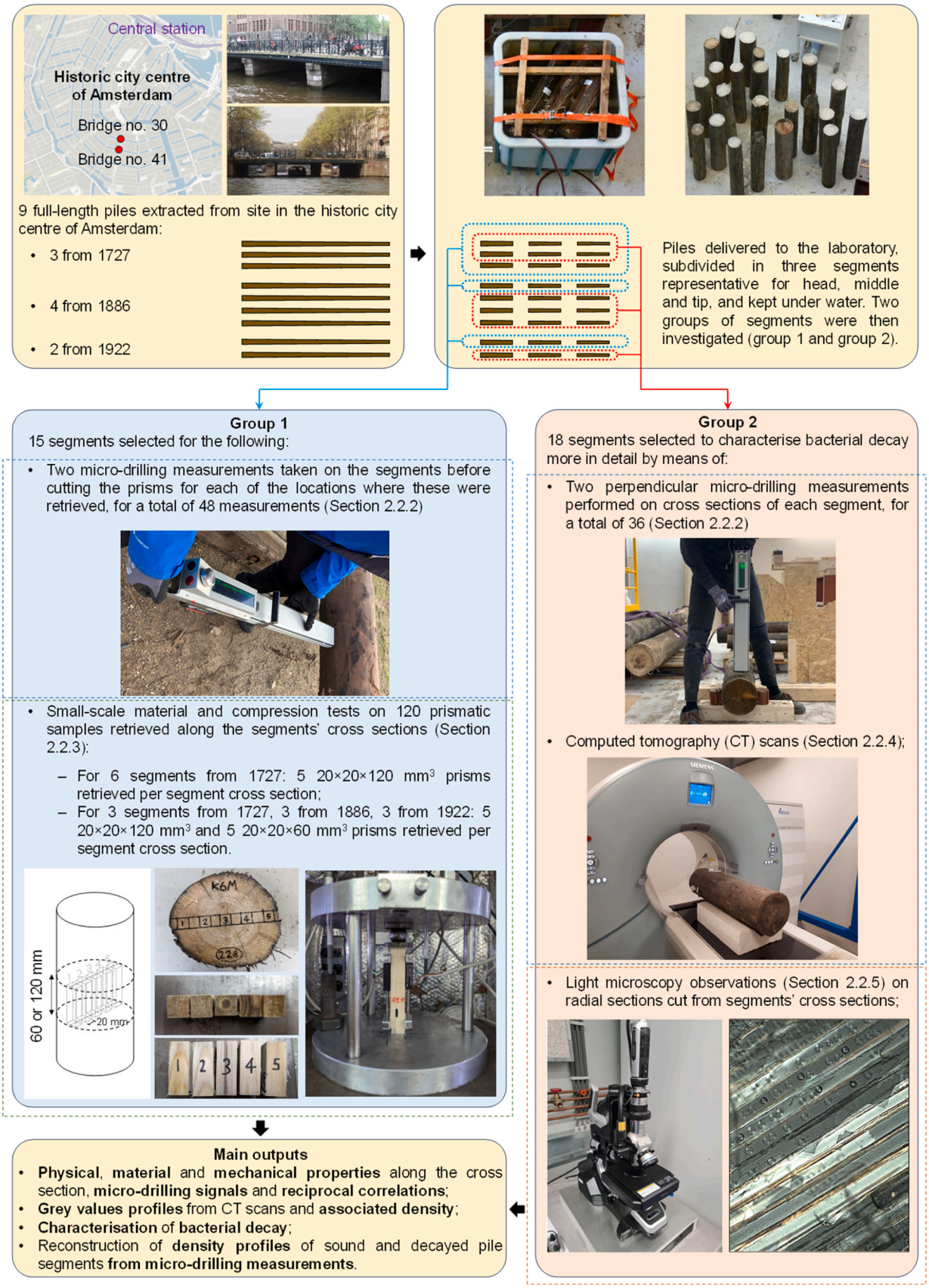

Fig. 1. Schematic representation of the methodology adopted for the present research study.

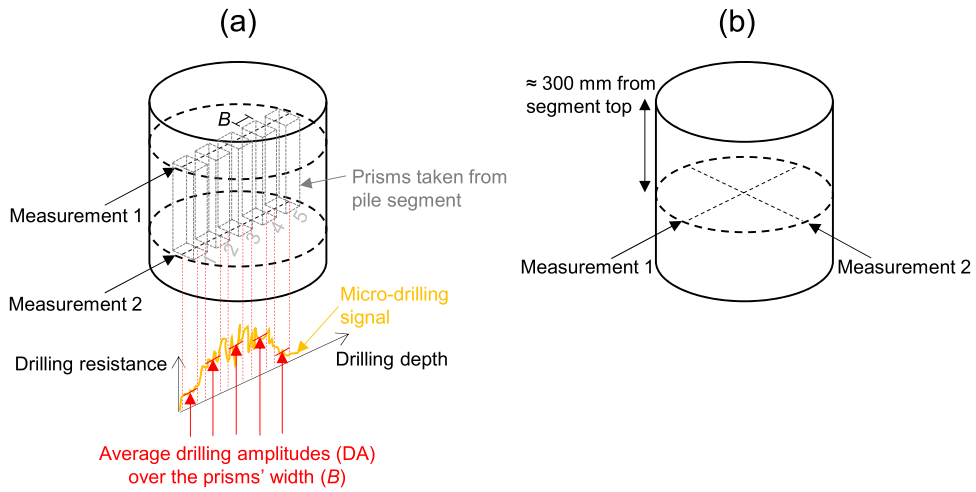

Fig. 2. Principle for execution of micro-drilling measurements across the grain for pile segments of group 1 (a) and group 2 (b).

section cause pronounced variations of strength, stiffness and moisture content, all factors ultimately influencing the global load-carrying capacity and service life of the piles: when bacterial decay progresses to the extent that most of the cell walls are eroded, a strong reduction of density and compressive strength occurs, linked to an increase in moisture content as well [1,6,19].

In the city of Amsterdam, spruce, pine, and occasionally fir piles, have been dominantly employed to realize foundation structures [1,19]. The local soil is mainly composed of peat and clay layers, resting on a sand layer at a depth of 11–12 m, and the groundwater is mainly brackish [19]. Given the essential function of these foundations and their widespread presence in the historic city centre of Amsterdam, estimating the remaining service life of the piles is crucial for arranging timely maintenance interventions.

To this end, an extensive experimental campaign has been started by the municipality of Amsterdam in cooperation with Delft University of Technology [20], aimed at characterising the current state of wooden foundation piles [21–23], as well as providing solid input for service life prediction models [24,25]. Among the available techniques for assessing the state of timber piles on site, micro-drilling measurements constitute a promising option [26–35], because with this method extensive in-situ sampling of a large number of piles can be efficiently conducted under water by divers [20–23,36,37]. Micro-drilling measurements can already be effectively adopted for qualitative assessment of (existing) timber structures [37], and they provide useful information on the state of wooden foundation piles' cross sections [22,23,25]. On this basis, investigating the possibility of using micro-drilling techniques also for a quantitative purpose in underwater conditions is of interest, especially in terms of the capability of correctly representing the aforementioned gradients in mechanical properties, caused by bacterial decay, along the cross section.

1.2. Research objectives and approach

A first objective of this work is the detailed characterisation, in terms of material and mechanical properties, of historic wooden piles from the city of Amsterdam, with specific reference to the influence of bacterial decay in their load-carrying capacity. The piles involved in this study (Section 2) have been exposed in the soil for 99, 135 and 294 years (with reference to 2021, year of extraction). Thus, it was possible to assess for which time in service of the piles the effects of degradation start influencing the mechanical properties. Several techniques at full-scale and small-scale level were adopted for this characterisation: compressive tests on prismatic samples retrieved from their cross sections, determination of their moisture content and density in water-submerged as well as dry conditions, micro-drilling measurements, computed tomography (CT) scans, and light microscopy observations (Section 2.2).

Because it is not possible to perform such a detailed assessment for wooden foundation piles on site, a second objective of this work is to assess the possibility of characterising the state of the piles by means of micro-drilling measurements. Correlations between the material and mechanical properties of the prisms and the micro-drilling signals were investigated, to check the reliability of micro-drilling measurements in identifying decay from both a qualitative and quantitative point of view. After presenting the methodology at the basis of this research work (Section 2), the results of the conducted tests are presented (Section 3), followed by their discussion (Section 4). Finally, in Section 5, the main conclusions are summarized.

2. Materials and methods

2.1. Materials

This research study involved 9 wooden foundation piles, fully submerged in water, and which were part of the foundation system of the piers of two bridges (catalogued as no. 30 and 41) 150 m far from each other in the city of Amsterdam (Fig. 1). According to the database of the Engineering Office of the Municipality of Amsterdam (*Ingenieursbureau Amsterdam*), the piles were dated back to 1727 (3 piles), 1886 (4 piles), and 1922 (2 piles). The length of the piles was ≈ 12 m, their head diameter ranged from 175 to 260 mm, while their tip diameter ranged from 125 to 210 mm. All piles were made of spruce (*Picea abies*), with the exception of one from 1886, made of fir (*Abies alba*).

2.2. Methods

2.2.1. General

After extraction, the piles were transported and delivered to TU Delft Stevin II Laboratory, where they were further subdivided in three segments representative for head, middle and tip part. The segments were coded in the form "year-number-pile part" (e.g. 1727–1-head), and were subdivided into two groups of specimens, hereinafter referred to as group 1 and group 2, for additional investigations (Fig. 1).

Group 1 consisted of 15 segments from 5 piles (Fig. 1): 9 segments from 1727, 3 from 1886, and 3 from 1922, all kept under water for two weeks to reproduce the on-site submerged conditions. The main target for the segments in group 1 was the characterisation of material and mechanical properties along the cross section for a disc taken from the segments, from which smaller longitudinal prismatic samples were retrieved: this was especially of interest for decayed piles, as the effects

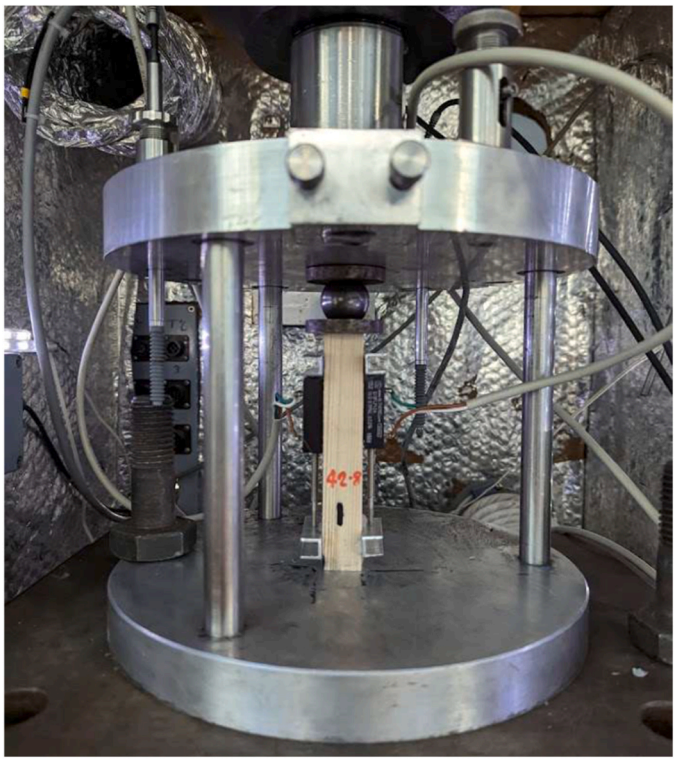

Fig. 3. Setup for compression tests of prisms.

of biodegradation on strength, stiffness and density could be quantified. For all segments, a location without knots was identified, and before cutting the prisms, two micro-drilling measurements were conducted in the same direction along which the prisms were taken within the cross section, right above and below the prisms themselves (Section 2.2.2 and Fig. 2). Next, five $20\times20\times120$ mm^3 prisms were retrieved from the cross section to test their material and mechanical properties (see Fig. 1 and Section 2.2.3), in agreement with EN 408 [38]. Additionally, for head, middle part and tip of samples 1727–1, 1886–1 and 1922–1, other 5 $20\times20\times60$ mm^3 prisms were taken, to assess whether a possible influence of size effect was present. In this way, it was possible to determine the physical, material and mechanical properties of the prisms, and to establish their correlations with micro-drilling measurements. A total of 120 prisms were tested, and 48 micro-drilling measurements were taken (Fig. 1).

In group 2 (18 segments), the main aim was a more detailed characterisation of bacterial decay. Group 2 also included six segments from 1727 which were part of group 1 (Fig. 1), to ensure a complete characterisation of the piles with the longest exposure time. From all segments, two micro-drilling measurements perpendicular to each other were taken (Section 2.2.2), and CT scans (Section 2.2.4), as well as light microscopy observations on thin radial sections retrieved from the cross section in correspondence to the micro-drilling measurements (Section 2.2.5), were performed. A total of 36 micro-drilling measurements and 18 CT scans were executed, and ≈ 100 radial sections were examined under the microscope. The outcomes from the tests performed on the segments of group 2 allowed to characterise their decay and main features, as well as to obtain their density profiles, retrieved from CT scans. As a final step, the reconstruction of density profiles by means of micro-drilling measurements was also evaluated, thus combining the outcomes of group 1 and group 2.

Table 1
Results from small-scale compression tests on prisms retrieved from 9 pile segments (3 head, 3 middle, 3 tip parts) from 1727.

Prism number	Number of samples	Presence of decay	Prism height (mm)	Moisture content at testing		Dry density		Compressive strength	
				Average (%)	Coefficient of variation	Average (kg/m^3)	Coefficient of variation	Average (MPa)	Coefficient of variation
1	9	Yes	120	216	0.37	304	0.13	8.2	0.64
2	9	No	120	89	0.23	439	0.03	12.0	0.18
3	9	No	120	62	0.23	402	0.02	10.1	0.31
4	9	No	120	63	0.39	439	0.03	13.2	0.01
5	9	Yes	120	212	0.50	358	0.32	8.4	0.63
1	3	Yes	60	146	0.57	315	0.19	7.5	0.31
2	3	No	60	52	0.34	436	0.14	13.8	0.15
3	3	No	60	60	0.10	403	0.04	10.8	0.18
4	3	No	60	58	0.37	452	0.02	13.7	0.06
5	3	Yes	60	189	0.43	351	0.32	8.6	0.64

Table 2
Results from small-scale compression tests on prisms retrieved from 3 pile segments (head, middle, tip) from 1886.

Prism number	Number of samples	Presence of decay	Prism height (mm)	Moisture content at testing		Dry density		Compressive strength	
				Average (%)	Coefficient of variation	Average (kg/m^3)	Coefficient of variation	Average (MPa)	Coefficient of variation
1	3	No	120	52	0.32	496	0.07	16.8	0.18
2	3	No	120	44	0.05	378	0.03	14.0	0.07
3	3	No	120	55	0.13	373	0.01	9.1	0.16
4	3	No	120	58	0.48	372	0.05	10.9	0.07
5	3	No	120	51	0.11	453	0.01	15.5	0.06
1	3	No	60	55	0.04	460	0.07	14.6	0.17
2	3	No	60	41	0.12	398	0.06	15.1	0.03
3	3	No	60	65	0.34	382	0.02	10.4	0.13
4	3	No	60	41	0.04	374	0.02	13.0	0.03
5	3	No	60	45	0.27	488	0.07	17.9	0.17

Table 3
Results from small-scale compression tests on prisms retrieved from 3 pile segments (head, middle, tip) from 1922.

Prism number	Number of samples	Presence of decay	Prism height (mm)	Moisture content at testing		Dry density		Compressive strength	
				Average (%)	Coefficient of variation	Average (kg/m^3)	Coefficient of variation	Average (MPa)	Coefficient of variation
1	3	No	120	120	0.19	487	0.01	14.8	0.12
2	3	No	120	46	0.20	510	0.05	19.1	0.13
3	3	No	120	49	0.17	460	0.11	13.5	0.17
4	3	No	120	59	0.43	499	0.01	19.8	0.13
5	3	No	120	143	0.17	428	0.07	13.9	0.14
1	3	No	60	117	0.29	436	0.13	13.5	0.22
2	3	No	60	74	0.57	503	0.09	21.4	0.36
3	3	No	60	44	0.10	489	0.12	17.1	0.14
4	3	No	60	61	0.30	502	0.10	19.1	0.16
5	3	No	60	111	0.15	450	0.10	14.5	0.32

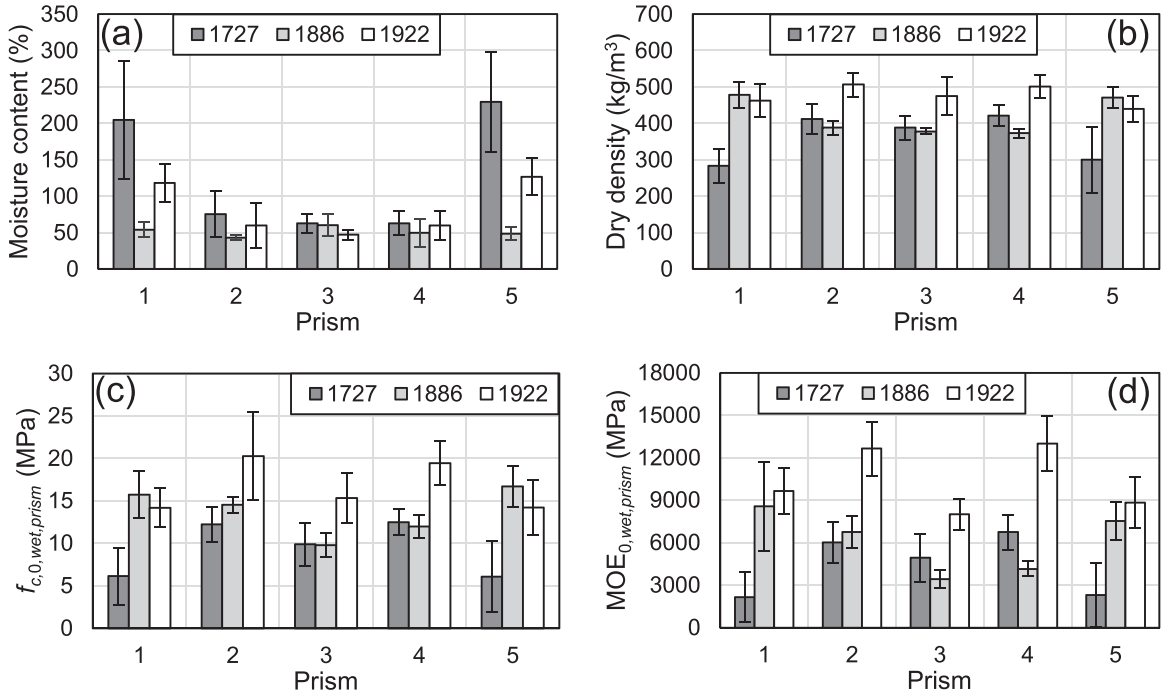

Fig. 4. Results from the small-scale experimental campaign on prisms retrieved along the cross sections of pile segments of group 1 (Section 2.2.3): (a) moisture content gradient; (b) dry density distribution; (c) wet compressive strength distribution; (d) wet modulus of elasticity distribution; average values and standard deviations are shown.

2.2.2. Execution of micro-drilling measurements

Micro-drilling measurements were performed for both groups of segments with an IML-RESI PD400 drill [39], shown in Fig. 1, according to the scheme illustrated in Fig. 2. This instrument provides the profiles of drill and feed amplitude against drilling depth as output [22]. A drill speed of 2500 r/min and a feed speed of 150 cm/min were adopted, in agreement with previous preliminary studies on wooden foundation piles [22,23]; the drill needle was 400 mm long, with a thin shaft of 1.5-mm diameter and a 3.1-mm-wide triangular cutting part, with hard chrome coating.

For the 15 segments of group 1, two measurements were taken across the grain in the cross sections above and below the prisms (Fig. 2a), and along the same radial orientation. This was done to avoid damage to the prisms, given their small dimensions [35]. For the 18 segments of group 2, two measurements were taken 300 mm below the top of each segment, in two orthogonal directions (Fig. 2b). Additionally, for group 1, the average drilling amplitude (DA) of the drilling resistance (DR) profiles along the width B of each prism (Fig. 2) was calculated as [23,37]:

$$\mathrm{DA} = \frac{\int_0^B \mathrm{DR}\ \mathrm{db}}{B} \quad (1)$$

For each prism, the calculated average DA over its width was then correlated with its material and mechanical properties.

2.2.3. Determination of material and mechanical properties of small-scale prismatic samples

For each segment in submerged conditions (moisture content > 50%), on one location over the length, five longitudinal prismatic samples were retrieved from the cross section: two corresponding to the outermost part (1 and 5, containing sapwood and possibly subjected to bacterial decay in the older samples), two containing heartwood (2 and 4), and one heartwood sample on the pith location (3, see Fig. 1). Following EN 384 [40], volume and weight of the prisms for deriving their wet density were subsequently measured by means of a calliper and a scale. Each prism was then tested in compression parallel to the grain following the protocol of EN 408 [38], adopting the displacement-controlled setup shown in Fig. 3. The prisms were placed

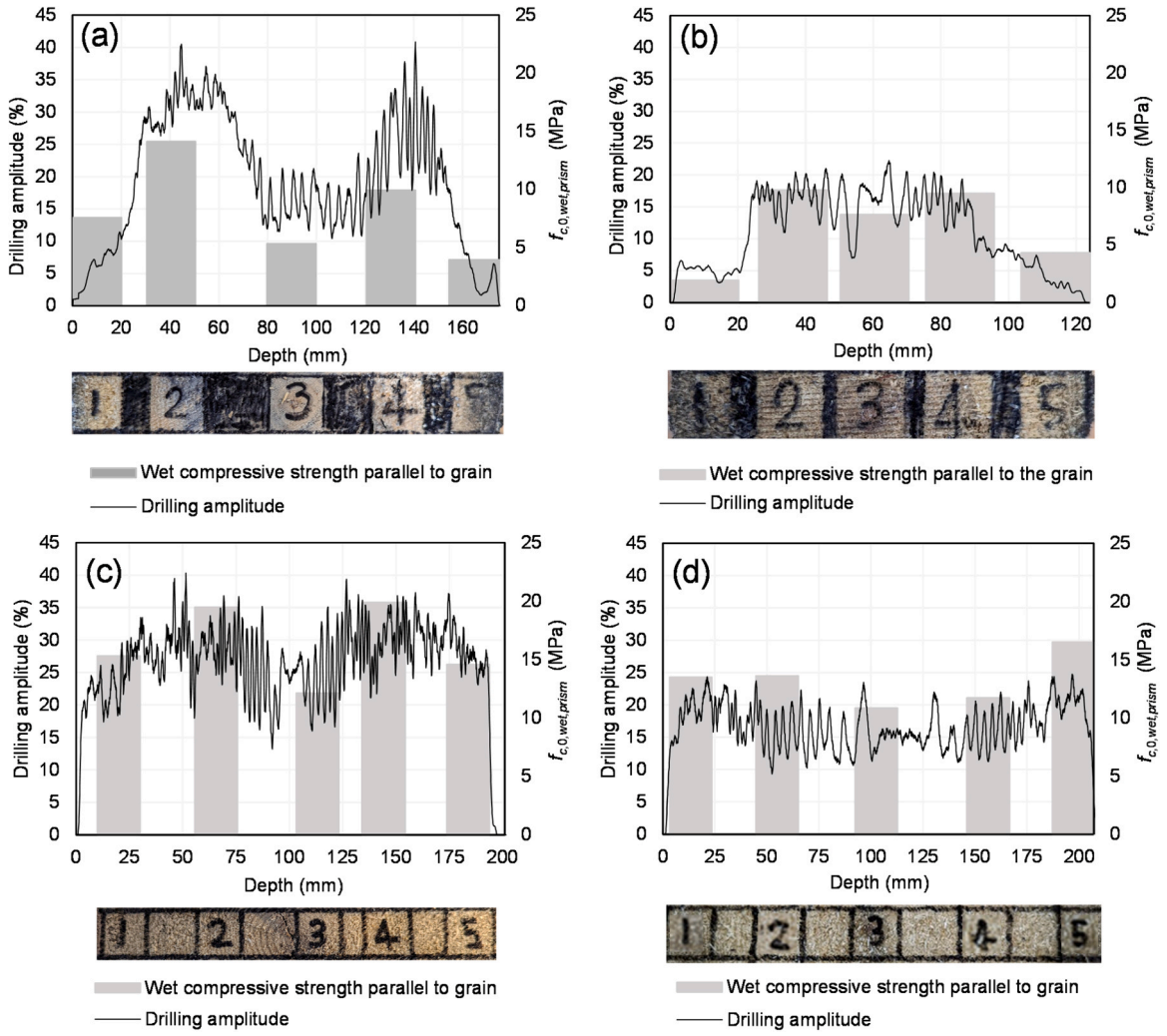

Fig. 5. Comparison between micro-drilling signals and wet compressive strength profiles of the prisms (Section 2.2.3) along the cross section for two representative decayed segments – 1727–1-head (a) and 1727–1-tip (b), and two sound ones – 1922–1-middle (c) and 1886–3-middle (d).

between two steel plates, and the application of a compressive load without inducing bending was ensured by means of a hinge. Besides the three potentiometers already present in the testing machine, other two were placed on opposite sides of the prisms. The tests were conducted at a displacement rate of 0.02 mm/s, and both compressive strength $f_{c,0,wet,prism}$ and modulus of elasticity $MOE_{0,wet,prism}$ parallel to the grain of the prisms were determined. Immediately after testing, the moisture content of the prisms was determined according to EN 13183–1 [41], as well as their dry density. In this way, from these experiments it was possible to reconstruct the density, strength, and stiffness profiles, as well as moisture content gradients along the cross sections of the segments.

2.2.4. Computed tomography (CT) scans

CT scans were performed for all 18 segments belonging to group 2, dried in indoor conditions for at least three months, in order to optimally capture the variations in measured dried density. To this end, a *Siemens Somatom Definition* CT scanner was used, with a 0.6 mm sampling resolution. In this way, images from the segments were retrieved from X-rays by measuring the reflected radiations; the obtained images are displayed in grey values reported in Hounsfield units (HU) [42], with water having a value of 0 HU, tissues denser than water having positive values, and tissues less dense than water having negative values [42], up to −1000 HU for air. When using grey values, low-density tissues appear as darker (blacker) and high-density structures as brighter (whiter) colours. With reference to wooden elements, this representation is associated with brighter colours in correspondence of e.g. knots, and darker colours around low-density or degraded areas [43].

In this way, the difference in densities in cross sections and in whole pile segments could be characterised and reconstructed. For the post-processing of the scans, conducted with *myVGL 2022.1* software [44], the grey values and associated dried densities were subdivided in ranges, each one of which was assigned a representative colour:

- Red for 90–180 kg/m^3
- Orange for 180–270 kg/m^3
- Yellow for 270–360 kg/m^3
- Green for 360–450 kg/m^3 (expected average reference for sound spruce/fir wood)
- Blue for 450–540 kg/m^3 (dense sound wood, or knots/compression wood)

Thus, the less dense decayed areas could appear as red-orange, the sound wood as green (or blue, for denser tissue). The obtained density profiles from the CT, were used to validate those predicted from the micro-drilling measurements on the same segments, on the basis of the correlations established from the tests on the segments of group 1 (Section 2.2.3).

2.2.5. Light microscopy observations

To complete the characterisation of biodegradation for the pile

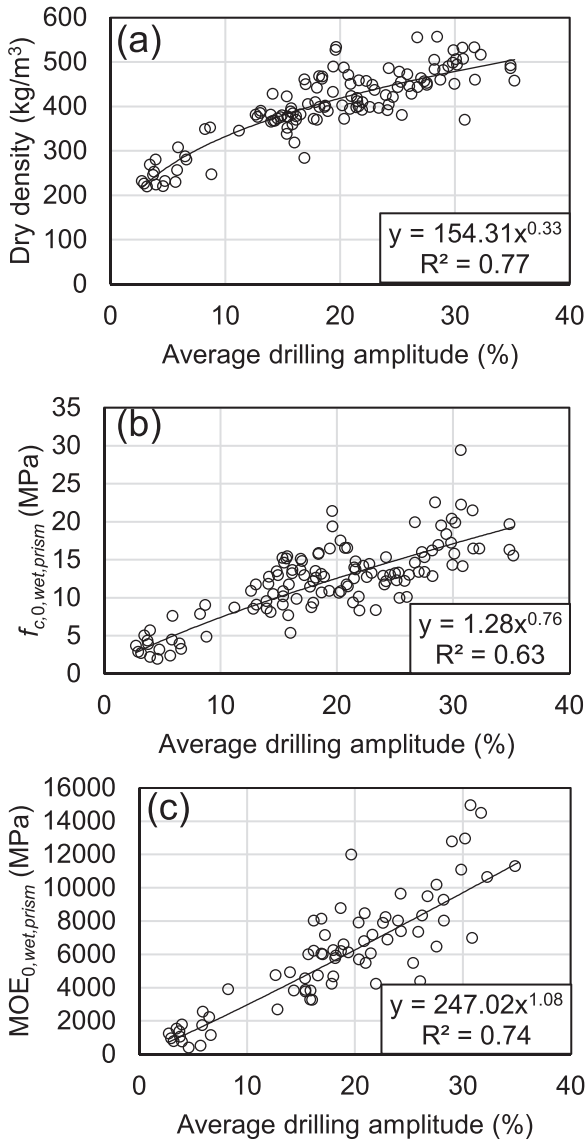

Fig. 6. Correlations derived from the small-scale experimental campaign on prisms retrieved along the cross sections of the pile segments of group 1: relationship between average drilling amplitude (DA) over the width B = 20 mm of each prism (Section 2.2.2) and their (a) dry density; (b) wet compressive strength, and (c) wet modulus of elasticity.

segments of group 2, light microscopy observations were performed as well. In this way, the extent of decay from the wood surface inwards was assessed. To this end, radial sections with a thickness of 20 μm suitable for microscopic observations were retrieved from the locations where micro-drilling measurements were executed. These radial sections were cut with a *Leica HistoCore Multicut R* microtome, and examined under polarised light with a *Keyence VHX 6000* digital microscope. The use of polarized light enabled the detection of birefringence, a typical feature of cellulose: once this is degraded by bacteria, a loss of birefringence is observed [1,4,6]. Bacterial decay was also evaluated by considering wood microanatomical features (presence of erosion channels, degraded cell walls), associated with corresponding decay levels, similarly to the classification provided in reference literature for wooden foundation piles [1,6]:

- No degradation: smooth cell walls, showing clear, intensive birefringence under polarised light [1];
- Light degradation: few degraded tracheids with small eroded grooves in earlywood; sound tracheids in latewood [1,6];
- Moderate degradation: diffuse degraded tracheids in a matrix of sound cells; in most earlywood tracheids, presence of erosion channels aligned along the micro-fibrils; in latewood tracheids, presence of typical diamond or v-shaped figures [1,6], not related to tracheid-ray connections;
- Severe degradation: few sound tracheids in a matrix of degraded cells; cell walls fully eroded, often filled with residual material; presence of erosion channels aligned along the micro-fibrils; no birefringence [1].

3. Results

3.1. Small-scale compression tests on prisms retrieved from the pile segments of group 1

The outcomes from the small-scale compression tests on prisms retrieved from group 1 pile segments, are reported in Table 1, Table 2, and Table 3 for prisms from 1727, 1886, and 1922, respectively. The results are shown separately for the two prisms' sizes (20×20×120 mm^3 and 20×20×60 mm^3), and the very small differences (10% on average) in the recorded parameters suggest that size effect does not influence the results from these tests; this outcome is in agreement with previous research work on spruce samples [45]. The graphical distributions of moisture content, dry density, wet compressive strength, and wet modulus of elasticity (the latter measured only for the 120-mm-high prisms) are shown in Fig. 4.

These findings indicate presence of decay for all segments from 1727, even though limited to the outer prisms (1 and 5): these show large moisture contents (up to 350%), as well as low dry density, compressive strength, and modulus of elasticity, whereas the other prisms (2, 3, 4) show values in line with those from more recent piles. Thus, a drop in load-carrying capacity of the most ancient piles can be expected, because of the poor material and mechanical properties of the outer portion of their cross section, the inner part remaining sound. However, although biological decay was absent in this inner portion, the presence of mechanical degradation cannot be a priori excluded, given the observable difference in properties between older (1886 and 1727) and more recent segments (1922).

The signals from the executed micro-drilling measurements were then compared with the variation of mechanical properties along the cross section of the piles: four representative examples are provided in Fig. 5 for two decayed and two sound segments. For the decayed segments from 1727 (Fig. 5a-b), a comparison is provided between head and tip of the same pile: it is interesting to notice how the micro-drilling signal is able to capture the decrease in mechanical properties within the cross section of the pile tip, mainly due to more extensive bacterial decay in prisms 1 and 5, and larger presence of juvenile wood in prisms 2 and 4, as compared to the head. In general, the drilling resistance profiles provide a reliable representation of the characteristics of the cross section, with the compressive strength of the single prisms following the same pattern as the measured amplitude. In particular, a clear identification of decayed portions was possible, and this was well in line with the results obtained from the tests on the prisms.

The latter statement is also supported by Fig. 6, showing the correlations between the average drilling amplitude measured within the width of the prisms, and their material and mechanical properties. In general, the low or very low drilling amplitudes found in the outer prisms (1 and 5 in Fig. 1, Fig. 4 and Fig. 5) are linked to low dry densities, compressive strength, and modulus of elasticity, and to large moisture contents, all features imputable to the effects of bacterial decay in the outer portion of the cross section. It should be noticed that the obtained correlations between the drilling amplitude and the strength and stiffness of the prismatic samples refer to clear wood, while the compressive failure of full piles may also occur because of whorl clusters

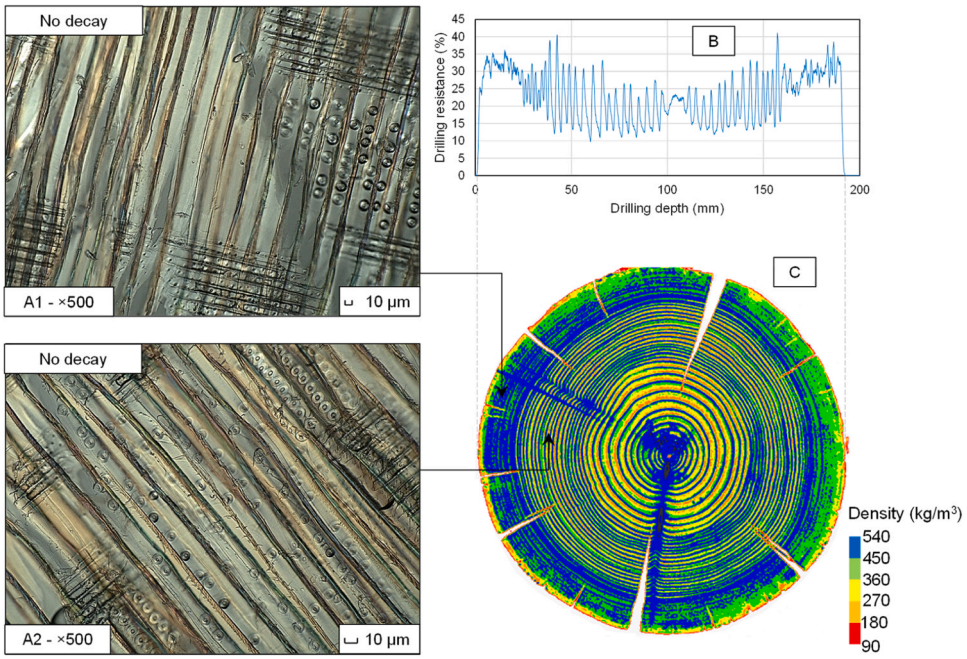

Fig. 7. Comparison between light microscopy observations (A1-A2, with reported magnification and scale) and micro-drilling signal (B) along the cross section of sample 1922–2-tip (sound spruce segment), and its corresponding CT scan (C). Smooth cell walls and intensive birefringence were observed, corresponding to the absence of decay (Section 2.2.5) in the examined radial sections (A1-A2), a result confirmed by micro-drilling and CT scan.

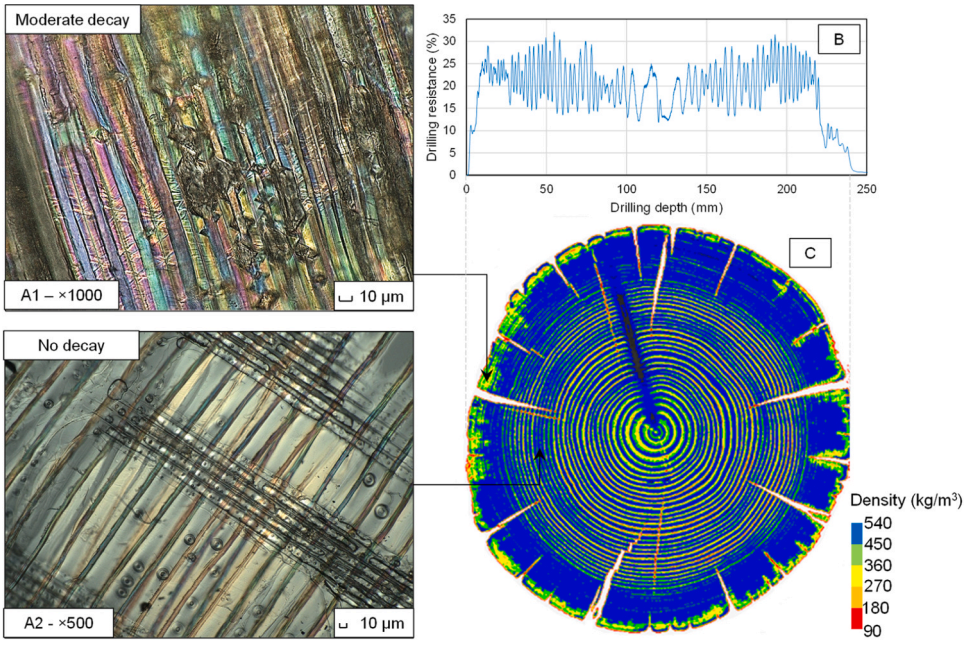

Fig. 8. Comparison between light microscopy observations (A1-A2, with reported magnification and scale) and micro-drilling signal (B) along the cross section of sample 1886–2-head (fir segment, incipient moderate decay in the very outer portion), and its corresponding CT scan (C). In radial section A1, a matrix of sound cells showing birefringence is observed, but with some tracheids showing darker triangular-shaped notches caused by bacterial degradation, corresponding to moderate decay (Section 2.2.5); radial section A2 featured no signs of decay: both results are confirmed by micro-drilling and CT scans.

[46]: further research will be conducted on the possibility of direct compressive strength prediction from micro-drilling signals by investigating a larger dataset; these investigations will be reported in future publications. The correlation with the dry density can instead be employed to reconstruct the density profile of a cross section along the drilling depth, and will be therefore validated in the following using the micro-drilling measurements conducted on the segments from group 2 (see Section 4).

3.2. CT scans, light microscopy observations, and micro-drilling measurements performed on pile segments of group 2

CT scans, light microscopy observations, and micro-drilling measurements performed on the 18 segments of group 2, are compared in this section. Among these pile segments, six from 1727 were also part of group 1, to fully characterise their state. The more recent pile segments from 1922 did not show biodegradation phenomena (Fig. 7); in few

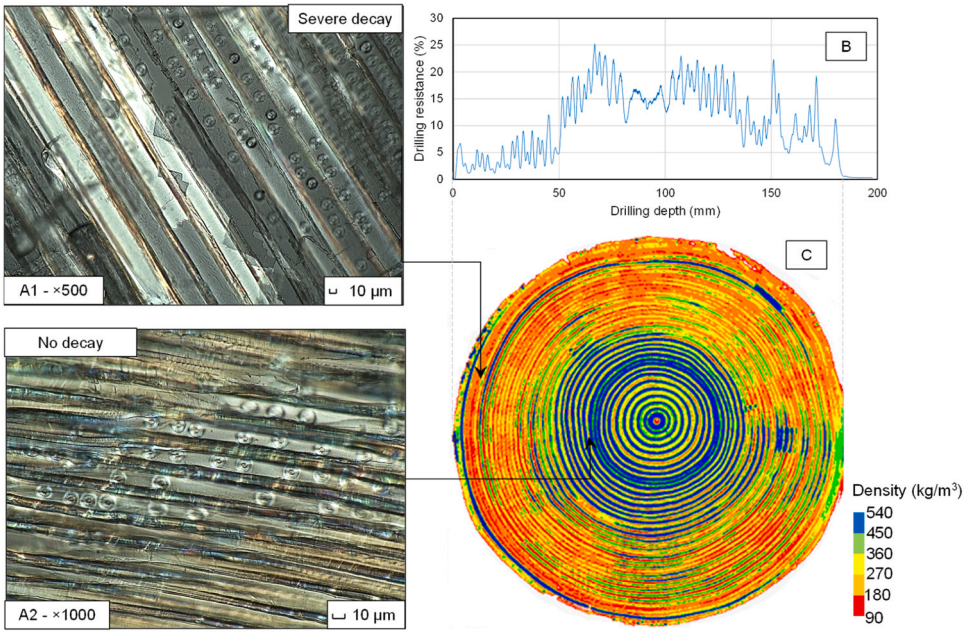

Fig. 9. Comparison between light microscopy observations (A1-A2, with reported magnification and scale) and micro-drilling signal (B) along the cross section of sample 1727–2-tip (spruce segment, severely decayed in the outer portion), and its corresponding CT scan (C). In radial section A1, only few sound cells showing birefringence are present, whereas the other tracheids are fully degraded and do not exhibit birefringence, corresponding to severe decay (Section 2.2.5); radial section A2 featured no signs of decay: both results are confirmed by micro-drilling and CT scans.

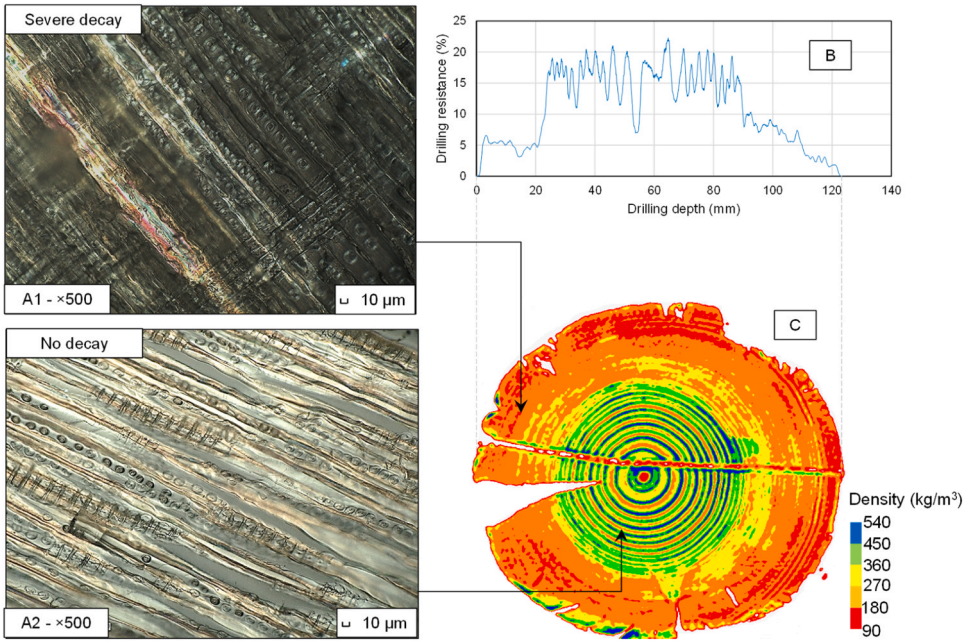

Fig. 10. Comparison between light microscopy observations (A1-A2, with reported magnification and scale) and micro-drilling signal (B) along the cross section of sample 1727–1-tip (spruce segment, severely decayed in the outer portion), and its corresponding CT scan (C). In radial section A1, only few sound cells showing birefringence are present, whereas the other tracheids are fully degraded and do not exhibit birefringence, corresponding to severe decay (Section 2.2.5); radial section A2 featured no signs of decay: both results are confirmed by micro-drilling and CT scans.

cases, incipient decay was found in 1886 segments (Fig. 8): both drilling resistance and density distribution from CT scans exhibited lower values on a very limited outer portion of the segment, where light microscopy observations revealed the presence of moderate decay as defined in Section 2.2.5. Most of the cells in the radial sections taken from the surface of the segments still showed birefringence (Fig. 8-A1), but several darker areas with the typical degradation pattern of erosion bacteria [1,4,6], were visible. The radial sections taken from the inner of the segments were intact, with smooth cell walls and intense birefringence (Fig. 8-A2).

A more critical situation was found in the segments from 1727 (Figs. 9–10), all featuring moderate to severe decay (Section 2.2.5) extending from their surface up to a depth of approximately 50 mm, as also confirmed by the very low drilling resistance and density distribution from CT scans. The corresponding radial sections observed under the microscope, featured erosion channels due to bacterial action, and

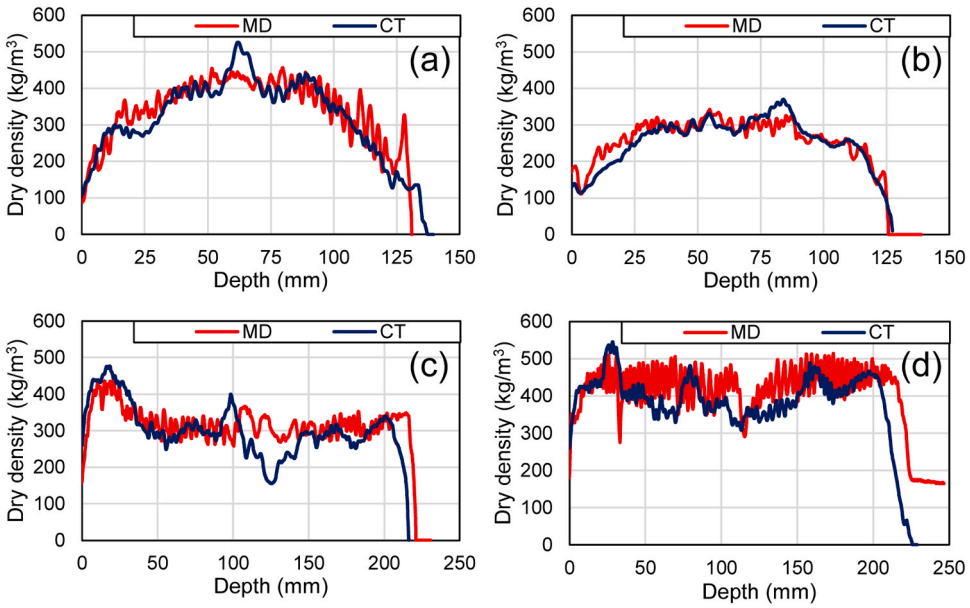

Fig. 11. Reconstruction of density profiles from micro-drilling (MD) measurements compared to those retrieved from CT scans for: two spruce decayed segments 1727–2-tip (a) and 1727–1-tip (b); sound spruce segment 1886–1-head featuring compression wood on the left side (c); sound fir segment 1886–2-head (d).

almost no birefringence under the microscope's polarized light, with only few sound cells left, indicating severe decay (Fig. 9-A1 and Fig. 10-A1). On the contrary, no evidence of decay was found in the radial sections taken from the inner of the segments (Fig. 9-A2 and Fig. 10-A2). This underpins the outcomes presented in Section 3.1, where the inner prisms (2, 3, 4) had properties in line with sound wood even in the most ancient samples.

4. Discussion

The results from small-scale compression tests, CT scans, microscopy observations, and micro-drilling measurements, show that the effects of bacterial decay were particularly evident in the piles with the longest service life: moderate to severe degradation was detected in the piles from 1727, affecting the outer 20–50 mm of their cross sections. In few cases, incipient degradation was found in 1886 samples, especially in tips. The observed degrees of degradation and the extension of decay within the piles' cross section are comparable to the outcomes from previous investigations on spruce, pine and fir piles in the Netherlands [1,19].

The small-scale tests performed on prisms (Section 3.1) allowed to quantify the impact of bacterial degradation on their material and mechanical properties. It was observed that prisms retrieved from locations affected by severe decay in 1727 segments, had large moisture contents (up to 350%), low basic densities (even less than 200 kg/m^3) and mechanical properties (average compressive strength of 6 MPa and average modulus of elasticity of less than 3000 MPa). Thus, compared to reference wet values for sound spruce roundwood [45], these prisms exhibited a more than doubled moisture content and halved mechanical properties, supporting and expanding on the findings in [1,19]. For the other prisms from sound 1886 and 1922 segments, better characteristics were found, comparable to the results of [45]. The obtained values refer to wet conditions, corresponding to a moisture content above fibre saturation point, since the piles are submerged in practice. Such wet parameters could also be related to the usual values at 12% moisture content, as further elaborated in [45].

The poor material and mechanical properties obtained in severely decayed areas of 1727 pile segments, were also linked to a very low drilling resistance resulting from micro-drilling measurements, and small density values detected with CT scans in these locations. Additionally, complete loss of birefringence at cellular level, proving the removal of cellulose due to erosion bacteria, as well as their typical degradation patterns [1,4,6,7], were observed under the microscope (Section 3.2). Yet, the inner of these piles did not show signs of decay and had properties in line with sound wood, once more proving the better resistance of heartwood against bacterial degradation, compared to sapwood [1,4,6,7,17,18].

Since the effects of decay could be well captured with micro-drilling measurements (Figs. 5, 7–10), a reconstruction of the cross section of the pile segments in terms of dry density is possible, because of the good relationship between this parameter and the drilling amplitude established with the small-scale tests on group 1 prisms (Section 3.1, Fig. 6a). The obtained equation was applied to the micro-drilling measurements conducted on the segments of group 2, and the resulting density profiles were compared to those retrieved from the CT scans along the path followed by the drill. The outcomes of this analysis are shown in Fig. 11: the density profiles could be successfully reconstructed for both decayed (Fig. 11a,b) and sound segments (Fig. 11c,d). Furthermore, for sample 1886–1-head (Fig. 11c), the presence of compression wood was observed in the left part of the cross section, and this specific feature could be accurately captured with the micro-drilling signal as well, showing a larger amplitude in that area.

5. Conclusions

In this work, an experimental campaign has been presented, aimed at characterising the effects of bacterial decay on wooden foundation piles supporting bridges in the historic city centre of Amsterdam (NL), from both the material and the mechanical point of view. The research study involved nine piles from different construction years (1727, 1886, 1922) extracted from site, and delivered to TU Delft Stevin II laboratory. The effects of bacterial decay were characterised by means of micro-drilling measurements, small-scale material and compressive tests on prismatic samples retrieved from the piles' cross sections, computed tomography scans on pile segments, and light microscopy observations.

The conducted investigations revealed that piles from 1922 and 1886 were mostly not affected by degradation, while moderate to severe decay was detected in 1727 piles, affecting the outer 20–50 mm of their cross section, where large moisture contents as well as poor material and mechanical properties were also observed. Additionally, it was

demonstrated that micro-drilling measurements are well correlated with such properties, providing both qualitative and quantitative information on the degradation state of the piles. In particular, the correlation established with the dry density was employed to accurately predict the density profiles of the piles' cross sections from micro-drilling signals, which were successfully validated against those obtained with the CT scans. For the direct prediction of compressive strength and modulus of elasticity of the piles on the basis of the micro-drilling signals, further research is envisaged to investigate possible correction factor to relate the predicted strength (referred to small-scale samples, i.e. clear wood) with the actual capacity of the pile, which could also be influenced by the presence of whorl clusters.

In this work, promising results were obtained in relation to the use of underwater micro-drilling measurements for in-situ monitoring of (ancient) wooden foundation piles. These outcomes have been supported by the unique opportunity to examine in detail samples dated back to different construction years and from the same location, adopting an integrated approach at different scales for their characterisation. The results of this study contribute to the research framework supporting testing and modelling methods for estimating decay, (residual) load-carrying capacity, and remaining service life of wooden foundation structures.

CRediT authorship contribution statement

Geert Ravenshorst: Writing – review & editing, Supervision, Project administration, Funding acquisition. **Jan-Willem van de Kuilen:** Writing – review & editing, Project administration, Funding acquisition. **Michele Mirra:** Writing – original draft, Visualization, Methodology, Investigation, Formal analysis, Data curation, Conceptualization. **Giorgio Pagella:** Writing – review & editing, Visualization, Methodology, Data curation. **Michael Lee:** Methodology, Investigation, Conceptualization. **Wolfgang Gard:** Writing – review & editing, Supervision, Funding acquisition, Conceptualization.

Declaration of Competing Interest

The authors declare that they have no known competing financial interests or personal relationships that could have appeared to influence the work reported in this paper.

Data availability

Data will be made available on request.

Acknowledgements

The Authors thankfully acknowledge the Municipality of Amsterdam (*Gemeente Amsterdam*) for having funded and supported this experimental campaign (grant CS2B08), and all staff members of TU Delft *Stevin II* and *Geoscience and Engineering* Laboratories.

References

[1] R.K.W.M. Klaassen, Bacterial decay in wooden foundation piles—patterns and causes: a study of historical pile foundations in the Netherlands, Int. Biodeterior. Biodegrad. (2008) 61.
[2] N. Macchioni, B. Pizzo, C. Capretti, Grading the decay of waterlogged archaeological wood according to anatomical characterisation, Int. Biodeterior. Biodegrad. 84 (2013) 54–64.
[3] R.K.W.M. Klaassen, J.G.M. Creemers, Wooden foundation piles and its underestimated relevance for cultural heritage, J. Cult. Herit. 13S (2012) S123–S128.
[4] A.P. Singh, Y.S. Kim, T. Singh, Bacterial degradation of wood, Secondary Xylem Biology, Chapter 9, 2016..
[5] I. Irbe, O. Bikovens, V. Fridrihsone, M. Dzenis, Impact of biodeterioration on structure and composition of waterlogged foundation piles from Riga Cathedral (1211 CE), Latvia, J. Archaeol. Sci. Rep. 23 (2019) 196.
[6] C.G. Björdal, J. Elam, Bacterial degradation of nine wooden foundation piles from Gothenburg historic city center and correlation to wood quality, environment and time in service, Int. Biodeterior. Biodegrad. (2021) 164.
[7] C.G. Björdal, Microbial degradation of waterlogged archaeological wood, J. Cult. Herit. 13 (3) (2012) 118–122.
[8] D.M. Holt, E.B. Jones, Bacterial degradation of lignified wood cell walls in anaerobic aquatic habitats, Appl. Environ. Microbiol. 46 (3) (1983) 722–727.
[9] Daniel, G.F., Nilsson, T. Ultrastructural Observations on Wood Degrading Erosion bacteria, IRG/WP/1283 the International Research Group on Wood Preservation, 1986.
[10] Y.S. Kim, A.P. Singh, Micromorphological characteristics of wood biodegradation in wet environments: a review, IAWA J. 21 (2) (2000) 135–155.
[11] J.B. Boutelje, A.F. Bravery, Observations of the bacterial attack of piles supporting a Stockholm building, J. Inst. Wood Sci. 20 (1968) 47–57.
[12] J.B. Boutelje, B. Göransson, Decay in wood constructions below the ground water table, Swed. J. Agric. Res. 5 (1975) 113–123.
[13] B.A. Jordan, Site characteristics impacting the survival of historic waterlogged wood: a review, Int. Bioterioration Biodegrad. 47 (2001) 47–54.
[14] D.J. Huisman, E.I. Kretschmar, N. Lamersdorf, Characterising physicochemical sediment conditions at selected bacterial decayed wooden pile foundation sites in the Netherlands, Germany, and Italy, Int. Biodeterior. Biodegrad. 61 (1) (2008) 117–125.
[15] A.P. Singh, A review of microbial decay types found in wooden objects of cultural heritage recovered from buried and waterlogged environments, J. Cult. Herit. 13S (2012) S16–S20.
[16] N.B. Pedersen, C.G. Björdal, P. Jensen, C. Felby, Bacterial Degradation of Archaeological Wood in Anoxic Waterlogged Environments, RSC Publishing, The Royal Chemical Society,, Cambridge, 2013.
[17] Grinda, M. Some experience with attack of microorganisms on wooden constructions supporting foundations of houses and bridges. IRG/WP 97-10232, The international research group on wood preservation, 1997.
[18] R.K.W.M. Klaassen, B.S. van Overeem, Factors that influence the speed of bacterial wood degradation, J. Cult. Herit. 13S (2012) S129–S134.
[19] Klaassen, R.K.W.M. (editor). Preserving cultural heritage by preventing bacterial decay of wood in foundation piles and archaeological sites, Final report EVK4-CT-2001-00043, BACPOLES project, Wageningen, The Netherlands, 2005. Available at: https://www.shr.nl/uploads/pdf-files/2005-0101-final-report-european-project-bacpoles.pdf.
[20] van de Kuilen, J.W.G., Beketova-Hummel, O., Pagella, G., Ravenshorst, G.J.P., Gard, W.F. An integral approach for the assessment of timber pile foundations. Paper 597, World Conference on Timber Engineering, Santiago, Chile, 2021.
[21] G. Pagella, M. Mirra, G.J.P. Ravenshorst, J.W.G. van de Kuilen, Influence of knots and density distribution on compressive strength of wooden foundation piles, Curr. Perspect. New Dir. Mech., Model. Des. Struct. Syst. (2022), https://doi.org/10.1201/9781003348443-277.
[22] Pagella, G., Ravenshorst, G.J.P., Gard, W.F., van de Kuilen, J.W.G. Characterization and assessment of the mechanical properties of spruce foundation piles retrieved from bridges in Amsterdam, in: Proceedings of the Fourth International Conference on Timber Bridges, Biel, Switzerland, 2022.
[23] Mirra, M., Pagella, G., Gard, W.F., Ravenshorst, G.J.P., van de Kuilen, J.W.G., Influence of moisture content on the assessment of decay levels by micro-drilling measurements in wooden foundation piles, in: Proceedings of the World Conference on Timber Engineering, Oslo, Norway, 2023. https://doi.org/10.52202/069179-0530.
[24] J.W.G. van de Kuilen, Service life modelling of timber structures, Mater. Struct. 40 (1) (2007) 151–161.
[25] Gard, W.F., Ravenshorst, G.J.P., van de Kuilen, J.W.G. Historical wooden pile foundations in Amsterdam: an integrated approach for the estimation of structural performance and residual service life, in: Proceedings of the International Conference on Structural Analysis of Historical Constructions (SAHC 2023), 1370-1382, 2023.
[26] F. Rinn, F.H. Schweingruber, E. Schar, Resistograph and X-ray density charts of wood comparative evaluation of drill resistance profiles and X-ray density charts of different wood species, Holzforschung 50 (4) (1996) 303–311.
[27] C. Ceraldi, V. Mormone, E. Russo-Ermolli, Resistographic inspection of ancient timber structures for the evaluation of mechanical characteristics, Mater. Struct. 34 (2001) 59–64.
[28] S. Imposa, G. Mele, M. Corrao, G. Coco, G. Battaglia, Characterization of decay in the wooden roof of the S. Agata Church of Ragusa Ibla (Southeastern Sicily) by means of Sonic tomography and resistograph penetration tests, Int. J. Archit. Herit. 8 (2) (2014) 213–223.
[29] T. Lechner, T. Nowak, R. Kliger, In situ assessment of the timber floor structure of the Skansen Lejonet fortification, Sweden, Constr. Build. Mater. 58 (2014) 85–93.
[30] H. Cruz, D. Yeomans, E. Tsakanika, N. Macchioni, A. Jorissen, M. Touza, M. Mannucci, P.B. Lourenço, Guidelines for on-site assessment of historic timber structures, Int. J. Archit. Herit. 9 (2015) 277–289.
[31] E. Sharapov, C. Brischke, H. Militz, E. Smirnova, Prediction of modulus of elasticity in static bending and density of wood at different moisture contents and feed rates by drilling resistance measurements, Eur. J. Wood Wood Prod. 77 (5) (2019) 833–842.
[32] J. Jaskowska-Lemańska, E. Przesmycka, Semi-destructive and non-destructive tests of timber structure of various moisture contents, Materials 14 (1) (2021) 96.
[33] E. Sharapov, C. Brischke, H. Militz, Effect of grain direction on drilling resistance measurements in wood, Int. J. Archit. Herit. 15 (2) (2021) 250–258.

[34] M. Brunetti, G. Aminti, M. Vicario, M. Nocetti, Density estimation by drilling resistance technique to determine the dynamic modulus of elasticity of wooden members in historic structures, Forests 14 (6) (2023) 1107.
[35] E. Sharapov, A. Korolev, S. Shlychkov, N.T. Mascia, Effect of drilling resistance measurement on residual load capacity of Scots pine (Pinus sylvestris L.), Eur. J. Wood Wood Prod. (2023).
[36] M. Humar, A. Balzano, D. Kržišnik, B. Lesar, Assessment of wooden foundation piles after 125 years of service, Forests 12 (2021) 143.
[37] T.P. Nowak, J. Jasieńko, K. Hamrol-Bielecka, In situ assessment of structural timber using the resistance drilling method – evaluation of usefulness, Constr. Build. Mater. 102 (2016) 403–415.
[38] EN 408. Timber structures - Structural Timber and Glued Laminated Timber - Determination of Some Physical and Mechanical Properties, CEN, Brussels, Belgium, 2010.
[39] ⟨https://www.iml-service.com/product/iml-powerdrill⟩. (Accessed 20 February 2024). 2024.
[40] EN 384. Structural timber – Determination of Characteristic Values of Mechanical Properties and Density, CEN, Brussels, Belgium, 2016.
[41] EN 13183-1. Moisture Content of A Piece of Sawn Timber - Part 1: Determination by Oven Dry Method, CEN, Brussels, Belgium, 2002.
[42] C. Freyburger, F. Longuetaud, F. Mothe, T. Constant, J.-M. Leban, Measuring wood density by means of X-ray computer tomography, Ann. For. Sci. 66 (8) (2009) 804.
[43] F. Longuetaud, F. Mothe, J.-M. Lebsan, A. Makela, Picea abies sapwood width: variations within and between trees, Scand. J. For. Res. 21 (1) (2007) 41–53.
[44] ⟨https://www.volumegraphics.com/en/products/myvgl.html⟩.
[45] S. Aicher, G. Stapf, Compressive strength parallel to the fiber of spruce with high moisture content, Eur. J. Wood Wood Prod. 74 (2016) 527–542.
[46] ISO 24294, Timber - Round and Sawn Timber - Vocabulary, International Organization for Standardization (ISO), 2021.